Research Article

Journal of PeptideScience

Received: 27 July 2010 Revised: 15 September 2010 Accepted: 18 October 2010 Published online in Wiley Online Library: 21 February 2011

(wileyonlinelibrary.com) DOI 10.1002/psc.1332

Effect of one D-Leu residue on right-handed helical -L-Leu-Aib- peptides in the crystal state

Yosuke Demizu,[a]* Mitsunobu Doi,[b] Yukiko Sato,[a] Masakazu Tanaka,[c] Haruhiro Okuda[a] and Masaaki Kurihara[a]*

Four diastereomeric-Leu-Leu-Aib-Leu-Leu-Aib-peptides, Boc-D-Leu-L-Leu-Aib-L-Leu-L-Leu-Aib-OMe (1), Boc-L-Leu-D-Leu-Aib-L-Leu-L-Leu-Aib-OMe (2), Boc-L-Leu-L-Leu-Aib-D-Leu-L-Leu-Aib-OMe (3), and Boc-L-Leu-L-Leu-Aib-L-Leu-D-Leu-Aib-OMe (4), were synthesized. The crystals of the four hexapeptides were characterized by X-ray crystallographic analysis. Two diastereomeric hexapeptides 1 and 2 having D-Leu(1) or D-Leu(2) were folded into right-handed (*P*) 3_{10}-helical structures, while peptide 3 having D-Leu(4) was folded into a turn structure nucleated by type III′ and I′ β-turns, and peptide 4 having D-Leu(5) was folded into a left-handed (*M*) 3_{10}-helical structure. Copyright © 2011 European Peptide Society and John Wiley & Sons, Ltd.

Keywords: amino acids; peptide; X-ray crystallographic analysis; conformation; secondary structure

Introduction

The *de novo* design of peptides and proteins is of extraordinary importance in the fields of biotechnology, nanotechnology, and medicinal chemistry. A variety of approaches to control the conformations of peptides have been investigated [1,2], and the incorporation of D-amino acids [3–9] and α, α-disubstituted α-amino acids [10–16] to peptide sequences is of vital importance to construct unique secondary structures. To date, we have studied the conformation of peptides composed of various α, α-disubstituted α-amino acids [17–27], and have recently reported that the attachment of α-aminoisobutyric acid (Aib) residues, which is the prototype of the α, α-disubstituted α-amino acids, to L-leucine-based hexapeptide (L-Leu-L-Leu-Aib-L-Leu-L-Leu-Aib) stabilized the right-handed (*P*) 3_{10}-helical structure [28]. Furthermore, new secondary structures such as helix, β-turn, and *S*-shape turn could be built by appropriate design of Leu-based hexapeptides containing two L-Leu, two D-Leu, and two Aib residues [29]. In this study, we investigated the preferred secondary structures of L-Leu-L-Leu-Aib-L-Leu-L-Leu-Aib peptides by substitution of an L-Leu residue with a D-Leu residue in the crystalline state. That is to say, we have designed and synthesized four diastereomeric hexapeptides, Boc-D-Leu-L-Leu-Aib-L-Leu-L-Leu-Aib-OMe (**1**), Boc-L-Leu-D-Leu-Aib-L-Leu-L-Leu-Aib-OMe (**2**), Boc-L-Leu-L-Leu-Aib-D-Leu-L-Leu-Aib-OMe (**3**), and Boc-L-Leu-L-Leu-Aib-L-Leu-D-Leu-Aib-OMe (**4**), and studied their preferred secondary structures in the crystalline state (Figure 1).

Materials and Methods

Synthesis and Characterization of Peptides

Preparation of peptides **1,2,3**, and **4** was performed by conventional solution-phase methods using a segment (coupled with trimer acid Boc-Leu-Leu-Aib-OH and trimer amine H-Leu-Leu-Aib-OMe) condensation strategy with *O*-benzotriazole-*N*,*N*,*N*′,*N*′-tetramethyluronium hexafluorophosphate (HBTU) and 1-HOBT as coupling reagents [30]. All compounds were purified by column chromatography on silica gel. The spectroscopic data of **1,2,3**, and **4** supported the following structures (Figure 2).

*Boc-D-Leu-L-Leu-Aib-L-Leu-L-Leu-Aib-OMe (**1**)*

Colorless crystals; Mp 218–220 °C (recryst. from MeOH/CH_2Cl_2); $[\alpha]^{24}_D = -12.4$ ($c = 0.5$, MeOH); IR (in $CDCl_3$ solution) 3281, 2956, 1654, 1528, 1220 cm^{-1}; ^1H NMR (400 MHz, $CDCl_3$) δ 7.52 (d, $J = 8.8$ Hz, 1H), 7.20 (br s, 1H), 7.18 (br s, 1H), 7.17 (br s, 1H), 6.65 (br s, 1H), 5.15 (d, $J = 6.0$ Hz, 1H), 4.34 (m, 1H), 4.18 (m, 1H), 3.98 (m, 1H), 3.85 (m, 1H), 3.71 (s, 3H), 1.50–1.82 (m, 24H), 1.45 (s, 9H), 0.86–1.01 (m, 24H); ESI(+) MS *m/z* 778 $[M + Na]^+$.

*Boc-L-Leu-D-Leu-Aib-L-Leu-L-Leu-Aib-OMe (**2**)*

Colorless crystals; Mp 151–153 °C (recryst. from MeOH/MeCN); $[\alpha]^{24}_D = +10.0$ ($c = 0.5$, MeOH); IR (in $CDCl_3$ solution) 3280, 2960, 1655, 1528, 1221 cm^{-1}; ^1H NMR (400 MHz, $CDCl_3$) δ 7.52 (d, $J = 10.4$ Hz, 1H), 7.35 (br s, 1H), 7.31 (br s, 1H), 7.21 (br s, 1H), 7.12 (d, $J = 6.0$ Hz, 1H), 5.09 (br s, 1H), 4.29 (m, 1H), 4.15 (m, 1H), 3.91 (m, 1H), 3.85 (m, 1H), 3.73 (s, 3H), 1.49–1.83 (m, 24H), 1.44 (s, 9H), 0.87–1.00 (m, 24H); ESI(+) MS *m/z* 778 $[M + Na]^+$.

*Boc-L-Leu-L-Leu-Aib-D-Leu-L-Leu-Aib-OMe (**3**)*

Colorless crystals; Mp 148–150 °C (recryst. from MeOH/MeCN); $[\alpha]^{24}_D = -24.6$ ($c = 0.5$, MeOH); IR (in $CDCl_3$ solution) 3282,

* *Correspondence to: Yosuke Demizu and Masaaki Kurihara, Division of Organic Chemistry, National Institute of Health Sciences, 1-18-1, Kamiyoga, Setagaya, Tokyo 158-8501, Japan. E-mail: demizu@nihs.go.jp; masaaki@nihs.go.jp*

a *Division of Organic Chemistry, National Institute of Health Sciences, 1-18-1, Kamiyoga, Setagaya, Tokyo 158-8501, Japan*

b *Osaka University of Pharmaceutical Sciences, Osaka 569-1094, Japan*

c *Graduate School of Biomedical Sciences, Nagasaki University, 1-14 Bunkyo-machi, Nagasaki 852-8521, Japan*

Journal of PeptideScience

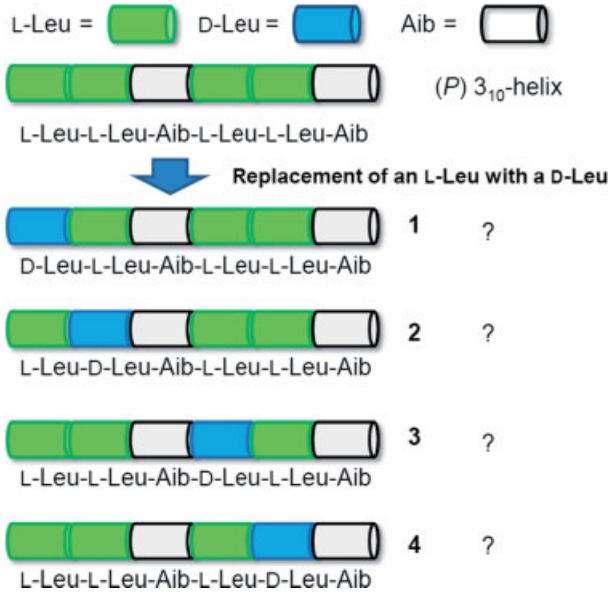

Figure 1. The design of diastereomeric hexapeptides **1, 2, 3**, and **4**.

2959, 1663, 1528, 1219 cm^{-1}; ^{1}H NMR (400 MHz, $CDCl_3$) δ 7.43 (d, J = 6.0 Hz, 1H), 7.17 (br s, 1H), 7.16 (br s, 1H), 7.05 (br s, 1H), 6.98 (br s, 1H), 5.42 (d, J = 5.2 Hz, 1H), 4.18 (m, 1H), 4.03 (m, 1H), 3.99 (m, 1H), 3.90 (m, 1H), 3.72 (s, 3H), 1.50–1.85 (m, 24H), 1.44 (s, 9H), 0.81–1.00 (m, 24H); ESI(+) MS m/z 778 $[M + Na]^+$.

*Boc-L-Leu-L-Leu-Aib-L-Leu-D-Leu-Aib-OMe (**4**)*

Colorless crystals; Mp 185–187 °C (recryst. from DMF/H_2O); $[\alpha]^{24}_D$ = −15.7 (c = 0.5, MeOH); IR (in $CDCl_3$ solution) 3296, 2957, 1657, 1526, 1263 cm^{-1}; ^{1}H NMR (400 MHz, $CDCl_3$) δ 7.46 (d, J = 7.6 Hz, 1H), 7.22 (br s, 1H), 7.15 (d, J = 7.6 Hz, 1H), 7.04 (br s, 1H), 6.64 (br s, 1H), 5.06 (br s, 1H), 4.28–4.32 (m, 2H), 4.03 (m, 1H), 3.88 (m, 1H), 3.69 (s, 3H), 1.45–1.83 (m, 24H), 1.43 (s, 9H), 0.85–1.03 (m, 24H); ESI(+) MS m/z 778 $[M + Na]^+$.

X-ray Diffraction

Peptides **1, 2, 3**, and **4** became good crystals for X-ray crystallographic analysis by slow evaporation of solvents MeOH/$CHCl_3$ for **1**, MeCN/MeOH for **2** and **3**, and DMF/H_2O for **4** at room temperature. The crystal and diffraction parameters of **1, 2, 3**, and **4** are summarized in Table 1. Data collection was performed on Bruker AXS SMART APEX imaging plate diffractometers using graphite-monochromated Mo$K\alpha$ radiation. All crystals remained stable during the X-ray data collection. The structures were solved using the SHELXS 97 direct method [31] and expanded by the Fourier technique [32]. All non-H atoms were given anisotropic thermal parameters, some H atoms were refined isotropically, and the remaining H atoms were given at the calculated positions. The final cycle of full-matrix least-squares refinement of **1** gave an R_1 factor of 0.0805 based on 10728 [$I > 2\sigma(I)$] reflections and an R_w factor of 0.1897 for all data. The R_1 factor of **2** was 0.0866 based on 10789 [$I > 2\sigma(I)$] reflections and an R_w factor of 0.2140 for all data. The R_1 factor of **3** was 0.0705 based on 5413 [$I > 2\sigma(I)$] reflections and an R_w factor of 0.2105 for all data. The R_1 factor of **4** was 0.0814 based on 4912 [$I > 2\sigma(I)$] reflections and an R_w factor of 0.2385 for all data [33]. Relevant backbone and side-chain torsion angles and the intra- and inter-molecular hydrogen-bond parameters are listed in Tables 2 and 3.

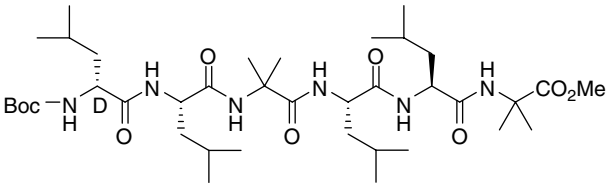

Boc-D-Leu-L-Leu-Aib-L-Leu-L-Leu-Aib-OMe (**1**)

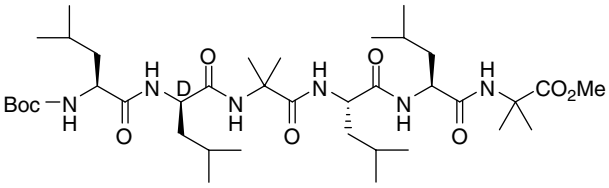

Boc-L-Leu-D-Leu-Aib-L-Leu-L-Leu-Aib-OMe (**2**)

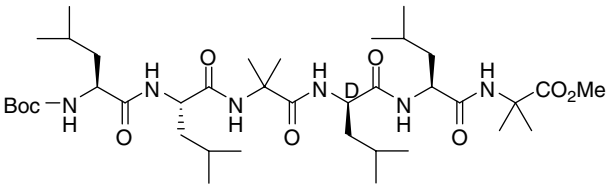

Boc-L-Leu-L-Leu-Aib-D-Leu-L-Leu-Aib-OMe (**3**)

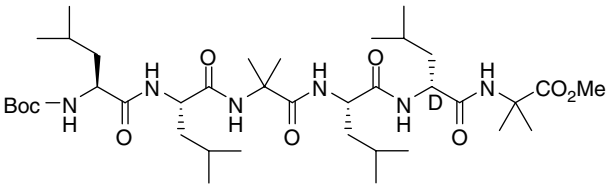

Boc-L-Leu-L-Leu-Aib-L-Leu-D-Leu-Aib-OMe (**4**)

Figure 2. Chemical structures of hexapeptides **1, 2, 3**, and **4**.

Results and Discussion

The X-ray analysis of Boc-D-Leu-L-Leu-Aib-L-Leu-L-Leu-Aib-OMe (**1**) was solved in the space group $P2_1$ to show a right-handed (P) 3$_{10}$-helical structure together with a chloroform molecule (Figure 3). The N-terminal D-Leu(1) and C-terminal ester group were flipped away from the helix. The mean values of the ϕ and ψ torsion angles of the residues [L-Leu(2) to L-Leu(5)] were −59.4 and −29.4°, which are close to those of an ideal right-handed (P) 3$_{10}$-helical structure (−60 and −30°) [34]. The flipped torsion angles (ϕ and ψ) at the N- and C-termini were positive, namely, +74.8°, +36.0° for the D-Leu(1), and +43.4°, +52.5° for the Aib(6) residues, respectively. In the crystal structure of **1**, three consecutive hydrogen bonds of the $i \leftarrow i + 3$ type between the H–N(4) and C(1)=O(1) [N(4)···O(1) = 2.97 Å; N–H···O 156.2°], the H–N(5) and C(2)=O(2) [N(5)···O(2) = 2.97 Å; N–H···O 160.7°], and the H–N(6) and C(3)=O(3) [N(6)···O(3) = 3.01 Å; N–H···O 131.4°] were observed. The chloroform molecule was fixed by a weak hydrogen bond between H–CCl_3 and O_0 [Cl_3C–O(0) = 3.06 Å; Cl_3C–H···O 136.4°] [35,36]. In the packing mode, two inter-molecular hydrogen bonds were observed between the H–N(1) donor and the C(4′)=O(4′) acceptor [N(1)···O(4′) = 2.91 Å; N–H···O 163.9°] of a symmetry-related molecule (1 + x, y, z), and the H–N(2) donor and the C(5′)=O(5′) acceptor [N(2)···O(5′) = 2.89 Å; N–H···O 141.0°] of a symmetry-related molecule (1 + x, y,

Table 1. Crystal and diffraction parameters of **1, 2, 3**, and **4**

	1	2	3	4
Formula	$C_{38}H_{70}O_9N_6$,$CHCl_3$	$C_{38}H_{70}O_9N_6$	$C_{38}H_{70}O_9N_6$	$C_{38}H_{70}O_9N_6$
Mr	874.37	755.00	755.00	755.00
Crystal dimensions (mm)	0.45 × 0.30 × 0.10	0.45 × 0.30 × 0.10	0.45 × 0.25 × 0.25	0.50 × 0.35 × 0.05
T (K)	240	240	240	240
Crystal system	Monoclinic	Triclinic	Orthorhombic	Monoclinic
a (Å)	11.273	10.436	19.665	11.071
b (Å)	20.867	11.056	23.092	19.270
c (Å)	11.819	21.940	10.521	11.841
α (°)	90	99.234	90	90
β (°)	114.054	91.590	90	112.593
γ (°)	90	91.454	90	90
V (Å^3)	2538.7	2496.5	4777.7	2332.2
Space group	$P2_1$	$P1$	$P2_12_12_1$	$P2_1$
Z value	2	2	2	2
D calc (g/cm^3)	1.144	1.004	1.050	1.075
μ (Mo$K\alpha$) (cm^{-1})	0.71	0.71	0.71	0.71
No. of observations [$I > 2\sigma(I)$]	10728	10789	5413	4912
No. of variables	514	955	478	478
R_1, R_w	0.0805, 0.1897	0.0866, 0.2140	0.0705, 0.2105	0.0814, 0.2385

Table 2. Selected torsion angles ω, ϕ, ψ, and χ (°) for **1, 2, 3**, and **4** as determined by X-ray crystallographic analysis

		2			
Torsion angle	1	Molecule **A**	Molecule **B**	3	4
ω0	170.8	−163.6	−161.5	174.2	−176.3
ϕ1	74.8	−64.2	−63.6	−87.4	−95.8
ψ1	36.0	−47.7	−47.4	−37.1	−27.1
ω1	176.5	−171.7	−172.1	174.9	179.8
ϕ2	−60.5	−59.5	−58.0	54.0	59.0
ψ2	−30.0	−33.9	−35.5	45.5	34.5
ω2	176.1	179.9	179.8	174.8	−176.2
ϕ3	−52.8	−54.2	−53.9	55.5	50.2
ψ3	−30.4	−36.7	−35.0	27.7	32.0
ω3	−176.7	−175.2	−174.8	174.8	178.2
ϕ4	−66.5	−72.4	−75.8	102.7	55.7
ψ4	−16.1	−15.7	−14.1	−9.1	28.9
ω4	171.8	171.8	171.4	178.8	−179.4
ϕ5	−57.7	−75.2	−76.6	−67.4	56.0
ψ5	−41.1	−37.4	−37.4	−29.2	38.9
ω5	174.3	−175.9	−175.9	−179.8	−175.0
ϕ6	43.4	46.7	46.7	50.5	−46.7
ψ6	52.5	47.5	48.4	48.2	−49.7
ω6	178.2	177.3	174.9	174.3	178.1
χ1	67.8	−173.3	−177.6	−56.9	−65.4
χ2	−63.3	56.5	57.1	−62.0	−50.6
χ4	−64.8	−55.8	−53.1	56.9	−51.5
χ5	−70.0	−178.5	−179.6	−69.1	74.3

z). The helical molecules were connected by two inter-molecular hydrogen bonds, forming head-to-tail alignment of chains, as shown in Figure 4. The flipping of D-Leu(1) may occur because of repulsion of the side chains between D-Leu(1) and L-Leu(5′) in the packing mode when the torsion angles of D-Leu(1) are negative.

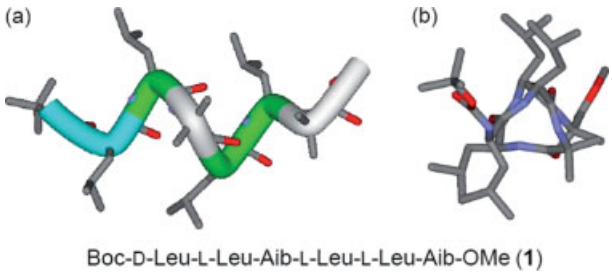

Figure 3. X-ray diffraction structures of **1** as viewed (a) perpendicular to and (b) along the helical axis. Chloroform molecule is omitted.

In the asymmetric unit of Boc-L-Leu-D-Leu-Aib-L-Leu-L-Leu-Aib-OMe (**2**), two right-handed (*P*) 3_{10}-helical structures were presented (Figure 5). The conformations of two molecules **A** and **B** were well matched, except for small differences in the conformation of the side chain, as shown by their superimposition in Figure 6. The mean values of the ϕ and ψ torsion angles of the residues were −65.1° and −34.3° for [L-Leu(1A) to L-Leu(5A)], and −65.6° and −33.9° for [L-Leu(1B) to L-Leu(5B)], which are close to those of an ideal right-handed (*P*) 3_{10}-helical structure. The reversal of the torsion angles occurred at the *C*-terminus, and the ϕ and ψ torsion angles (+46.7° and +47.5°) for the Aib(6A) and (+46.7° and +48.4°) for the Aib(6B) were positive, while those of the preceding residues were negative. In molecule **A**, two consecutive hydrogen bonds of the $i \leftarrow i+3$ type between the H–N(4A) and C(1A)=O(1A) [N(4A)···O(1A) = 2.91 Å; N–H···O 142.3°] and between the H–N(5A) and C(2A)=O(2A) [N(5A)···O(2A) = 2.99 Å; N–H···O 146.9°] were observed. Furthermore, one weak intra-molecular hydrogen bond between the H–N(6A) and C(3A)=O(3A) [N(6A)···O(3A) = 3.21 Å; N–H···O 131.7°] was observed. Molecule **B** similarly showed two intra-molecular hydrogen bonds between the H–N(4B) and C(1B)=O(1B) [N(4B)···O(1B) 2.87 Å; N–H···O 144.7°] and between the H–N(5B) and C(2B)=O(2B) [N(5B)···O(2B) 3.01 Å; N–H···O

Journal of PeptideScience

Table 3. Intra- and inter-molecular H-bond parameters for the peptides **1, 2, 3**, and **4**[a]

Donor D–HA	Acceptor A	Distance D···A	Angle (°) D–H···A	Symmetry operations
Boc-D-Leu-L-Leu-Aib-L-Leu-L-Leu-Aib-OMe (**1**)				
N_4–H	O_1	2.97	156.2	x, y, z
N_5–H	O_2	2.97	160.7	x, y, z
N_6–H	O_3	3.01	131.4	x, y, z
CCl_3-H	O_0	3.06	136.4	x, y, z
N_1–H	$O_{4'}$	2.91	163.9	$1 + x, y, z$
N_2–H	$O_{5'}$	2.89	141.0	$1 + x, y, z$
Boc-L-Leu-D-Leu-Aib-L-Leu-L-Leu-Aib-OMe (**2**)				
Molecule A				
N_{4A}–H	O_{1A}	2.91	142.3	x, y, z
N_{5A}–H	O_{2A}	2.99	146.9	x, y, z
N_{6A}–H	O_{3A}	3.21[b]	131.7	x, y, z
N_{1A}–H	$O_{4A'}$	2.84	153.8	$x, 1 + y, z$
N_{2A}–H	$O_{5A'}$	2.89	149.0	$x, 1 + y, z$
Molecule B				
N_{4B}–H	O_{1B}	2.87	144.7	x, y, z
N_{5B}–H	O_{2B}	3.01	148.2	x, y, z
N_{6B}–H	O_{3B}	3.29[b]	129.8	x, y, z
N_{1B}–H	$O_{4B'}$	2.87	159.6	$x, 1 + y, z$
N_{2B}–H	$O_{5B'}$	2.88	149.7	$x, 1 + y, z$
Boc-L-Leu-L-Leu-Aib-D-Leu-L-Leu-Aib-OMe (**3**)				
N_4–H	O_1	3.00	151.9	x, y, z
N_5–H	O_2	2.96	164.0	x, y, z
N_3–H	O_6	3.30b	162.5	x, y, z
N_1–H	$O_{5'}$	2.86	140.4	$1/2 + x, 1/2 - y, 1 - z$
N_2–H	$O_{5'}$	3.02	166.0	$1/2 + x, 1/2 - y, 1 - z$
N_3–H	$O_{6'}$	2.99	142.3	$1/2 + x, 1/2 - y, 1 - z$
Boc-L-Leu-L-Leu-Aib-L-Leu-D-Leu-Aib-OMe (**4**)				
N_4–H	O_1	2.85	150.8	x, y, z
N_5–H	O_2	2.93	160.2	x, y, z
N_6–H	O_3	3.02	135.6	x, y, z
N_1–H	$O_{4'}$	2.83	145.8	$1 + x, y, z$
N_2–H	$O_{5'}$	2.81	138.8	$1 + x, y, z$

[a] The number of the amino-acid residues begins at the *N*-terminus of the peptide.
[b] The distance of D···A is somewhat long for a hydrogen bond.

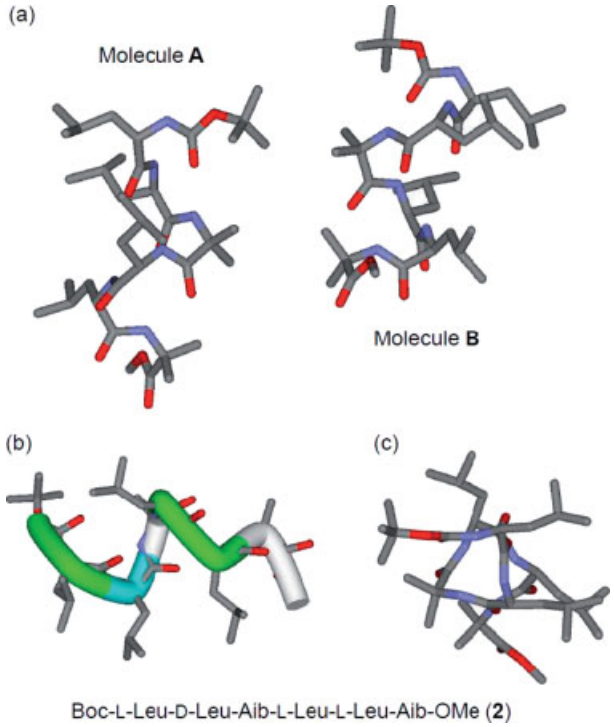

Figure 5. X-ray diffraction structures of **2** (a), and structure of molecule **A** as viewed (b) perpendicular to and (c) along the helical axis.

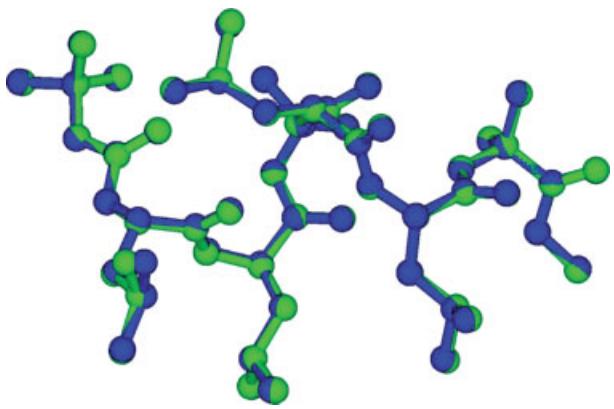

Figure 6. Overlay of the structures of molecules **A** (green) and **B** (blue).

148.2°], and additionally one weak intra-molecular hydrogen bond between the H–N(6B) and C(3B)═O(3B) [N(6B)···O(3B) = 3.29 Å; N–H···O 139.8°]. In the packing mode, four inter-molecular hydrogen bonds were observed between the H–N(1A) donor and the C(4A′)═O(4A′) acceptor [N(1A)···O(4A′) = 2.84 Å; N–H···O 153.8°] of a symmetry-related molecule (x, $1 + y$, z), the H–N(2A) donor and the C(5A′)═O(5A′) acceptor [N(2A)···O(5A′) = 2.89 Å; N–H···O 149.0°] of a symmetry-related molecule (x, $1 + y$, z), the H–N(1B) donor and the C(4B′)═O(4B′) acceptor [N(1B)···O(4B′) = 2.87 Å; N–H···O 159.6°] of a symmetry-related molecule (x, $1 + y$, z), and the H–N(2B) donor and the C(5B′)═O(5B′) acceptor

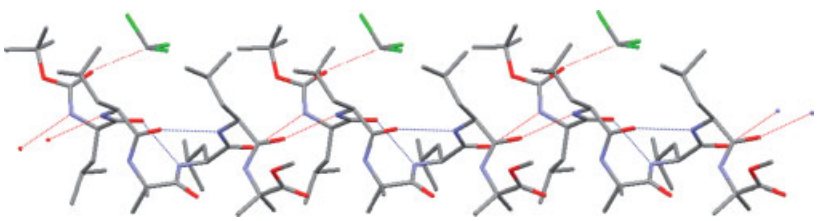

Figure 4. Packing of **1** in the crystalline state. Intra-molecular (blue) and inter-molecular (red) hydrogen bonds are indicated as dashed lines.

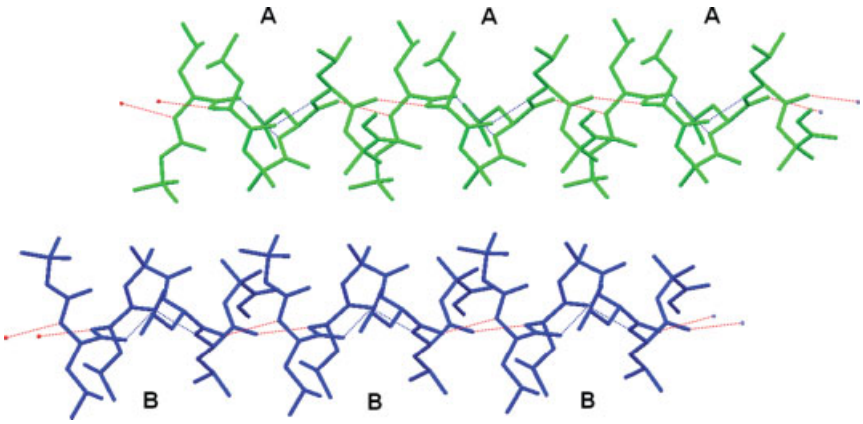

Figure 7. Packing of **2** (green for molecule **A** and blue for molecule **B**) in the crystalline state. Intra-molecular (blue) and inter-molecular (red) hydrogen bonds are indicated as dashed lines.

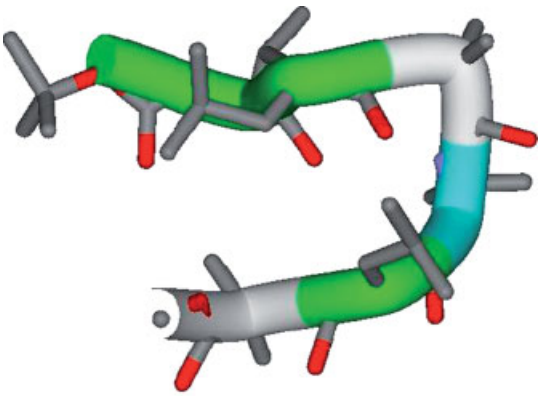

Boc-L-Leu-L-Leu-Aib-D-Leu-L-Leu-Aib-OMe (**3**)

Figure 8. X-ray diffraction structure of **3**.

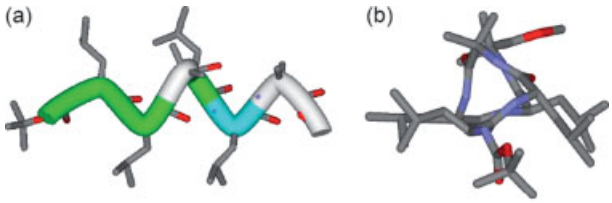

Boc-L-Leu-L-Leu-Aib-L-Leu-D-Leu-Aib-OMe (**4**)

Figure 10. X-ray diffraction structures of **4** as viewed (a) perpendicular to and (b) along the helical axis.

[N(2B)···O(5B′) = 2.88 Å; N–H···O 149.7°] of a symmetry-related molecule (x, $1 + y$, z). The two helical molecules **A** and **B** were connected by two inter-molecular hydrogen bonds, forming head-to-tail alignment of chains **-A-A-A-A-** and **-B-B-B-B-** (Figure 7).

Interestingly, the crystal structure of Boc-L-Leu-L-Leu-Aib-D-Leu-L-Leu-Aib-OMe (**3**) was solved in the space group $P2_12_12_1$ to show a β-turn structure nucleated by type III′ and I′ β-turns (Figure 8). The type III′ β-turn was formed between L-Leu(2) and Aib(3), and the values of the ϕ and ψ torsion angles of L-Leu(2) were $+54.0^\circ$ and $+45.5^\circ$, and those of Aib(3) were $+55.5^\circ$ and $+27.7^\circ$, respectively [backbone torsion angles of ideal type III′ β-turn: $\phi(i+1) = +60^\circ$, $\psi(i+1) = +30^\circ$, and $\phi(i+2) = +60^\circ$, $\psi(i+2) = +30^\circ$] [37]. The type I′ β-turn was formed between Aib(3) and D-Leu(4), and the values of the ϕ and ψ torsion angles of Aib(3) were $+55.5^\circ$ and $+27.7^\circ$, and those of D-Leu(4) were $+102.7^\circ$ and -9.1°, respectively, which were close to those of ideal type I′ β-turn [$\phi(i+1) = +60^\circ$, $\psi(i+1) = +30^\circ$, and $\phi(i+2) = +90^\circ$, $\psi(i+2) = 0^\circ$] [37]. In the crystal structure of **3**, two intra-molecular hydrogen bonds of the $i \leftarrow i+3$ type were observed between the H–N(4) and C(1)=O(1) [N(4)···O(1) = 3.00 Å; N–H···O 151.9°] and the H–N(5) and C(2)=O(2) [N(5)···O(2) = 2.96 Å; N–H···O 164.0°]. Furthermore, one weak intra-molecular hydrogen bond of the $i \leftarrow i+5$ type was observed between the H–N(6) and C(1)=O(1) [N(6)···O(1) = 3.30 Å; N–H···O 162.5°]. In the packing mode, three inter-molecular hydrogen bonds were observed between the H–N(1) donor and the C(5′)=O(5′) acceptor [N(1)···O(5′) =

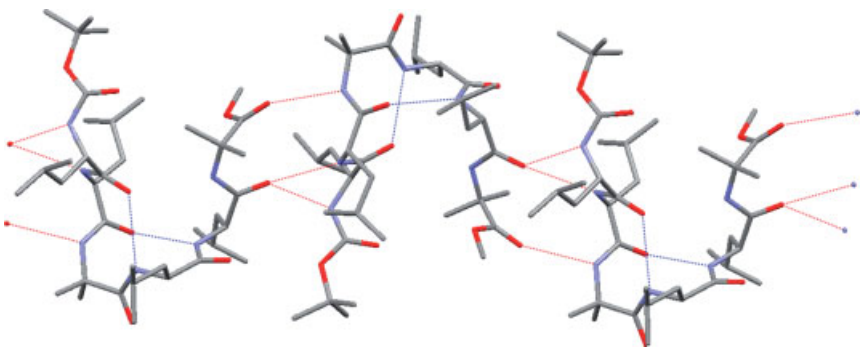

Figure 9. Packing of **3** in the crystalline state. Intra-molecular (red) and inter-molecular (blue) hydrogen bonds are indicated as dashed lines.

Journal of PeptideScience

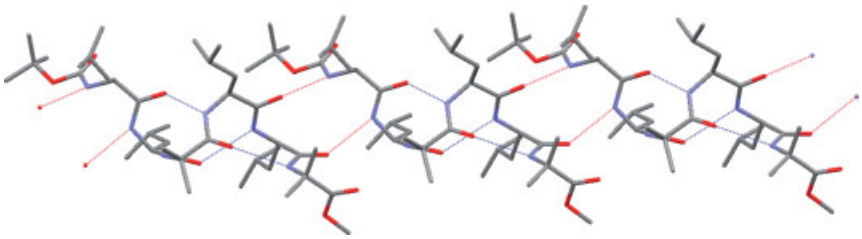

Figure 11. Packing of **4** in the crystalline state. Intra-molecular (red) and inter-molecular (blue) hydrogen bonds are indicated as dashed lines.

2.86 Å; N–H···O 140.4°] of a symmetry-related molecule ($1/2+x$, $1/2-y$, $1-z$), the H–N(2) donor and the C(5′)═O(5′) acceptor [N(2)···O(5′) = 3.02 Å; N–H···O 166.0°] of a symmetry-related molecule ($1/2+x$, $1/2-y$, $1-z$), and the H–N(3) donor and the C(6′)═O(6′) acceptor [N(3)···O(6′) = 2.99 Å; N–H···O 142.3°] of a symmetry-related molecule ($1/2+x$, $1/2-y$, $1-z$) (Figure 9). Two type β-turns (type I′ and III′) are consecutive, and the replacement of the L-Leu-L-Leu-Aib-L-Leu-L-Leu-Aib sequence with D-Leu(4) strongly influenced the peptide secondary structure to induce a left-handed turn.

Boc-L-Leu-L-Leu-Aib-L-Leu-D-Leu-Aib-OMe (**4**) was solved in the space group $P2_1$, and folded into a left-handed (*M*) 3_{10}-helical structure with flipping of *N*-terminal Leu(1) and *C*-terminal ester group (Figure 10). The mean values of the ϕ and ψ torsion angles of the residues [L-Leu(2) to D-Leu(5)] were +55.2° and +33.6°, respectively, which are close to those of an ideal left-handed (*M*) 3_{10}-helical structure (+60° and +30°) [34]. The torsion angles (ϕ and ψ) at the *N*- and *C*-termini were negative, namely, −95.8°, −27.1° for the L-Leu(1), and −46.7°, −49.7° for the Aib(6) residues, respectively. In the crystal structure of **4**, three consecutive hydrogen bonds of the $i \leftarrow i+3$ type were observed between the H–N(4) and C(1)═O(1) [N(4)···O(1) = 2.85 Å; N–H···O 150.8°], the H–N(5) and C(2)═O(2) [N(5)···O(2) = 2.93 Å; N–H···O 160.2°], and the H–N(6) and C(3)═O(3) [N(6)···O(3) = 3.02 Å; N–H···O 135.6°]. Two inter-molecular hydrogen bonds were observed between the H–N(1) donor and the C(4′)═O(4′) acceptor [N(1)···O(4′) = 2.83 Å; N–H···O 145.8°] of a symmetry-related molecule ($1+x$, y, z), and the H–N(2) donor and the C(5′)═O(5′) acceptor [N(2)···O(5′) = 2.81 Å; N–H···O 138.8°] of a symmetry-related molecule ($1+x$, y, z). The helical molecules were connected by two inter-molecular hydrogen bonds, forming head-to-tail alignment of chains, as shown in Figure 11. It should be noted that the hexapeptide **4** having only one D-Leu in the three L-Leu sequence crystallized into a left-handed (*M*) 3_{10}-helical structure. It has been reported that an *N*-terminal chiral amino acid would have stronger propensity to control the helical-screw sense of the achiral peptide than a *C*-terminal chiral one in solution [38,39]. However, the results showed that a *C*-terminal amino-acid residue could also be important for the control of helical-screw sense of the chiral peptide backbone in the crystal state.

Conclusions

Four diastereomeric hexapeptides **1, 2, 3**, and **4** of the L-Leu-L-Leu-Aib-L-Leu-L-Leu-Aib- sequence, in which an L-Leu residue is substituted with a D-Leu residue, were prepared and their conformations in the crystal state were analyzed by X-ray diffraction. In the crystal state of **1** with D-Leu(1) and **2** with D-Leu(2), a right-handed (*P*) 3_{10}-helical structure existed. Interestingly, the preferred conformation of **3** with D-Leu(4) was a β-turn structure nucleated by type III′ and I′ β-turns. Furthermore, that of **4** with D-Leu(5) was a left-handed (*M*) 3_{10}-helical structure. The replacement of the L-Leu-L-Leu-Aib-L-Leu-L-Leu-Aib sequence with D-Leu(1) or D-Leu(2) residues did not have a significant effect on the right-handed helical-screw sense. However, the D-Leu(4) and D-Leu(5) residues in peptides **3** and **4** had great influences on the peptide secondary structures to induce left-handed helical-screw sense in the crystal state. It is not clear why peptides **3** and **4** having one D-amino acid within the sequence of three L-amino acids preferentially formed type III′/I′ β-turns and the left-handed 3_{10}-helix. One reason may be that a slightly energetically favorable conformer is preferentially packed in the crystal state. These results will be of relevance to researchers investigating the control of secondary structures of peptides and rational design of peptidomimetics.

Acknowledgements

This work was supported in part by a Grant-in-Aid for Young Scientists (B) (21790018) from the Ministry of Education, Science, Sports, and Culture of Japan, and the Kurata Memorial Hitachi Science and Technology Foundation.

References

1 Schneider JP, Kelly JW. Template that induce α-helical, β-sheet, and loop conformations. *Chem. Rev.* 1995; **95**: 2169–2187.
2 Venkatraman J, Shankaramma SC, Balaram P. Design of folded peptides. *Chem. Rev.* 2001; **101**: 3131–3152.
3 Narita M, Honda S, Ueyama H. Conformational analysis of oligo-L-leucines containing only one D-amino acid residue. *Bull. Chem. Soc. Jpn.* 1987; **60**: 4127–4131.
4 Di Blasio B, Benedetti E, Pavone V, Pedone C, Spiniello O, Lorenzi GP. Regularly alternating L,D-peptides. I. The double-stranded left-handed antiparallel β-helix in the structure of Boc-(L-Val-D-Val)$_4$-OMe. *Biopolymers* 1989; **28**: 193–201.
5 Imperiali B, Moats RA, Fisher SL, Prins TJ. A conformational study of peptides with the general structure Ac-L-Xaa-Pro-D-Xaa-L-Xaa-NH$_2$. *J. Am. Chem. Soc.* 1992; **114**: 3182–3188.
6 Haque TS, Little JC, Gellman SH. Stereochemical requirements for β-hairpin formation: medel studies with four-residue peptides and depsipeptides. *J. Am. Chem. Soc.* 1996; **118**: 6975–6985.
7 Fabiola F, Pattabhi V, Rawale S, Raju EB, Durani S. Configurationally guided peptide conformational motifs: crystal structure of a L^{α} D^{β} L^{β} D^{α} D^{β} L^{α} type hexapeptide fold. *Chem. Commun.* 1997; 1379–1380.
8 Dhanasekaran M, Fabiola F, Pattabhi V, Durani S. A rationally designed turn-helix peptide. *J. Am. Chem. Soc.* 1999; **121**: 5575–5576.
9 Karle IL, Hosahudya GN, Balaram P. Crystal structure of a hydrophobic 19-residue peptide helix containing three centrally located D-amino acids. *Proc. Natl. Acad. Sci. U.S.A.* 2003; **100**: 13946–13951.
10 Jaun B, Tanaka M, Seiler P, Kuhnle FNM, Braun C, Seebach D. Studies on the conformation of Boc-protected (*S*)-(+)-isovaline homopeptide methyl esters in the solid state and in solution. *Liebigs Ann. Recl.* 1997; 1697–1710.
11 Karle IL. Controls exerted by the Aib residue: helix formation and helix reversal. *Biopolymers (Pept. Sci.)* 2001; **60**: 351–365.

12 Dehner A, Planker E, Gemmecker G, Broxterman QB, Bisson W, Formaggio F, Crisma M, Toniolo C, Kessler H. Solution structure, dimerization, and dynamics of a lipophilic $\alpha/3_{10}$-helical, C^{α}-methylated peptide. Implications for folding of membrane proteins. *J. Am. Chem. Soc.* 2001; **123**: 6678–6686.
13 Toniolo C, Crisma M, Formaggio F, Peggion C, Broxterman QB, Kaptein B. Molecular spacers for physicochemical investigations based on novel helical and extended peptide structures. *Biopolymers (Pept. Sci.)* 2004; **76**: 162–176.
14 Crisma M, Formaggio F, Moretto A, Toniolo C. Peptide helices based on α-amino acids. *Biopolymers (Pept. Sci.)* 2006; **84**: 3–12.
15 Aravinda S, Shamala N, Balaram P. Aib residues in peptaibiotics and synthetic sequences: analysis of nonhelical conformations. *Chem. Biodivers.* 2008; **5**: 1238–1262.
16 Ousaka N, Inai Y, Kuroda R. Chain-terminus triggered chiral memory in an optically inactive 3_{10}-helical peptide. *J. Am. Chem. Soc.* 2008; **130**: 12266–12267.
17 Oba M, Tanaka M, Kurihara M, Suemune H. Conformation of peptides containing (*S*-α-ethylleucine. *Helv. Chim. Acta* 2002; **85**: 3197–3218.
18 Tanaka M, Nishimura S, Oba M, Demizu Y, Kurihara M, Doi M, Suemune H. C_5 conformation and a 3_{10}-helical structure of peptide composed of diverse α-ethylated α,α-disubstituted α-amino acids. *Chem. Eur. J.* 2003; **9**: 3082–3090.
19 Tanaka M, Demizu Y, Doi M, Kurihara M, Suemune H. Chiral centers in the side chains of α-amino acids control the helical screw sense of peptides. *Angew. Chem. Int. Ed.* 2004; **43**: 5360–5363.
20 Royo S, Borggraeve WMD, Peggion C, Formaggio F, Crisma M, Jiménez AI, Cativiela C, Toniolo C. Turn and helical peptide handedness governed exclusively by side-chain chiral centers. *J. Am. Chem. Soc.* 2005; **127**: 2036–2037.
21 Tanaka M, Anan K, Demizu Y, Kurihara M, Doi M, Suemune H. Side-chain chiral centers of amino acid and helical-screw handedness of its peptides. *J. Am. Chem. Soc.* 2005; **127**: 11570–11571.
22 Tanaka M. Design and synthesis of chiral α,α-disubstituted α-amino acids and conformational study of their oligopeptides. *Chem. Pharm. Bull.* 2007; **55**: 349–358.
23 Nagano M, Tanaka M, Doi M, Demizu Y, Kurihara M, Suemune H. Helical-screw directions of diastereoisomeric cyclic α-amino acid oligomers. *Org. Lett.* 2009; **11**: 1135–1137.
24 Benedetti E, Saviano M, Iacovino R, Pedone C, Santini A, Crisma M, Formaggio F, Toniolo C, Broxterman QB, Kamphuis J. Helical screw sense of peptide molecules: the pentapeptide system $(Aib)_4$/L-Val[L-(αMe)Val] in the crystal state. *Biopolymers* 1998; **46**: 433–443.
25 Demizu Y, Yamagata N, Sato Y, Doi M, Tanaka M, Okuda H, Kurihara M. Controlling the helical screw sense of peptides with *C*-terminal L-valine. *J. Pept. Sci.* 2010; **16**: 153–158.
26 Oba M, Demizu Y, Yamagata N, Sato Y, Doi M, Tanaka M, Suemune H, Okuda H, Kurihara M. Solid-state conformation of diastereomeric -Pro-Pro- sequences. *Tetrahedron* 2010; **66**: 2293–2296.
27 Demizu Y, Tanaka M, Doi M, Kurihara M, Okuda H, Suemune H. Conformations of peptides containing a chiral cyclic α,α-disubstituted α-amino acid within the sequence of Aib residues. *J. Pept. Sci.* 2010; **16**: 621–626.
28 Demizu Y, Tanaka M, Nagano M, Kurihara M, Doi M, Maruyama T, Suemune H. Controlling 3_{10}-helix and α-helix of short peptides in the solid state. *Chem. Pharm. Bull.* 2007; **55**: 840–842.
29 Demizu Y, Doi M, Sato Y, Tanaka M, Okuda H, Kurihara M. Three-dimensional control of diastereomeric Leu-Leu-Aib-Leu-Leu-Aib sequences in the solid state. *J. Org. Chem.* 2010; **75**: 5234–5239.
30 Nagano M, Doi M, Kurihara M, Suemune H, Tanaka M. Stabilized α-helix-catalyzed enantioselective epoxidation of α,β-unsaturated ketones. *Org. Lett.* 2010; **12**: 3564–3566.
31 Sheldrick GM. *SHELXL 97. Program for Crystal Structure Refinement*. University of Göttingen: Göttingen, 1997.
32 Beurskens PT, Admiraal G, Beurskens G, Bosman WP, de Gelder R, Israel R, Smits JMM. *The DIRDIF-99 program system, technical report of the crystallography laboratory*, University of Nijmegen: The Netherlands, 1994.
33 CCDC-770819 for **1**, CCDC-770820 for **2**, CCDC-770821 for **3**, and CCDC-770822 for **4** contain the supplementary crystallographic data for this paper. These data can be obtained free of charge it via www.ccdc.cam.ac.uk/conts/retrieving.html. (or from the Cambridge Crystallographic Data Centre, 12, Union Road, Cambridge CB2 1EZ, UK; fax: (+44) 1223-336-033; or deposit@ccdc.cam.ac.uk).
34 Toniolo C, Benedetti E. The polypeptide 3_{10}-helix. *Trends Biochem. Sci.* 2000; **16**: 350–353.
35 Steiner T. Donor and acceptor strengths in C–H–O hydrogen bonds quantified from crystallographic data of small solvent molecules. *New J. Chem.* 1998; **22**: 1099–1103.
36 Desiraju GR. The C–H–O hydrogen bond in crystals. *Acc. Chem. Res.* 1991; **24**: 290–296.
37 Venkatachalam CM. Stereochemical criteria for polypeptides and proteins. V. Conformation of a system of three linked peptide units. *Biopolymers* 1968; **6**: 1425–1436.
38 Inai Y, Ishida Y, Tagawa K, Takasu A, Hirabayashi T. Noncovalent domino effect on helical screw sense of chiral peptides possessing *C*-terminal chiral residue. *J. Am. Chem. Soc.* 2002; **124**: 2466–2473.
39 Solà J, Helliwell M, Clayden J. *N*- versus *C*-terminal control over the screw-sense preference of the configurationally achiral, conformationally helical peptide motif $Aib_8GlyAib_8$. *J. Am. Chem. Soc.* 2010; **132**: 4548–4549.

